

# Serial Electron Microscopy as an Alternative or Complement to Confocal Microscopy for the Study of Synapses and Dendritic Spines in the Central Nervous System

**Kristen M. Harris**

Department of Neurology, and  
Program in Neuroscience  
The Children's Hospital, and  
Harvard Medical School  
Boston, Massachusetts

- I. Introduction
  - II. Series Sample Analysis
    - A. Serial Electron Microscopy
    - B. Quantitative Series Sample Analysis
    - C. Summary of Results That Have Benefited from Either Partial or Complete Series Sample Analysis
  - III. Three-Dimensional Reconstruction from Serial Electron Microscopy
    - A. Sources of Error in Three-Dimensional Reconstructions
    - B. Three-Dimensional Reconstructions of Individual Dendritic Spines and Synapses
    - C. Three-Dimensional Reconstructions of Dendritic Segments Coursing through Neuropil
    - D. Summary of Results from Three-Dimensional Reconstructions of Dendritic Spines and Synapses
    - E. Implications of Spine Dimensions and Three-Dimensional Characteristics for Spine Function
  - IV. Summary and Cautions
- References

## I. INTRODUCTION

Interest in dendritic spine and synaptic structure has been motivated by the effect that changes in their number, location, composition, and dimensions can have on interneuronal communication. Cajál first described dendritic spines as Stacheln and Dornen, which refer to the longer spic-

ule-like spines and shorter thornlike spines, using light microscopy of Golgi-impregnated neurons (Ramón Y Cajál, 1893, p. 343). It required electron microscopy (EM), however, to establish unequivocally that dendritic spines are the major postsynaptic targets of excitatory synapses in the central nervous system (Gray, 1959). Although fortuitous sections and viewing angles have allowed the shape of spines to be identified as "stubby," "mushroom," or "thin," depending on the constriction of their necks and the size of their heads (Peters and Kaiserman-Abramof, 1962; Jones and Powell, 1969), most spines cannot be recognized by shape on a single EM section or in light microscopy (Harris *et al.*, 1992). Furthermore, neither fortuitous thin sections nor light microscopy reveals the elaborately branched dendritic spines that have multiple heads and synapses; reconstruction through serial EM has always been required to elucidate the complex geometry and subcellular constituents of these spines (Hamlyn, 1962; Blackstad and Kjaerheim, 1961; Harris and Stevens, 1988, 1989; Chicurel and Harris, 1989).

Since the days of Cajál, it has been widely believed that learning and memory may require anatomical changes in neurons (Ramón Y Cajál, 1893; Tanzi, 1893; Wallace *et al.*, 1991). Modern theoretical models have focused this interest on how changes in the morphology of synapses and dendritic spines could alter synaptic function (Rall, 1970, 1974, 1977, 1978; Diamond *et al.*, 1970; Kawato and Tsukahara, 1983; Brown *et al.*, 1988; Wickens, 1988; Coss and Perkel, 1985; Segev and Rall, 1988; Turner, 1988; Koch and Poggio, 1983; Gamble and Koch, 1987; Wilson, 1984; Baer and Rinzel, 1991). There are essentially two categories of morphological change that could modulate physiological properties at synapses: either existing synapses could be modified pre- and/or postsynaptically, or new synapses and spines could be formed. Presynaptically, a change in the number or size of neurotransmitter-containing vesicles or in the number or location of release sites could affect the quantity or availability of neurotransmitter for release on activation of the presynaptic axon. Modifications in the size or shape of the postsynaptic receptive area could alter the number and density of receptors and other molecules involved in synaptic transmission. Changes in spine neck dimensions could alter their resistance to charge transfer from the synapse to the postsynaptic cell (Rall, 1970, 1974; Coss and Perkel, 1985; Brown *et al.*, 1988). The degree of spine neck constriction could also modulate transient calcium concentrations occurring near to synapses on spine heads following synaptic transmission (Gamble and Koch, 1987; Zador *et al.*, 1990; Muller and Connor, 1991). Spine neck constriction may determine whether the potential reached in the head of the spine is sufficient to activate voltage-dependent channels such as the calcium channel associated with the NMDA receptor (Gamble and Koch, 1987;

Wickens, 1988; Zador *et al.*, 1990). In addition, changes in the frequency and distribution of spines with different geometries could alter the postsynaptic integration of multiple synaptic inputs. Thus, quantitative descriptions of changes in synaptic number and location, vesicle number, position, or size, postsynaptic density (PSD) morphology, and spine dimensions are crucial for understanding the properties of synaptic transmission and quantal events at central synapses (Redman, 1990).

Indeed, several results suggest that the number and structure of dendritic spines change during development, learning, memory, and long-term potentiation; furthermore, spines appear distorted in pathological conditions associated with seizures, impaired memory, and mental retardation (for review, see Scheibel and Scheibel, 1968; Purpura, 1974, 1975a,b; Schuz, 1978; Greenough and Bailey, 1988; Harris *et al.*, 1989; Desmond and Levy, 1990; Wallace *et al.*, 1991). To discern whether individual spines undergo remodeling requires that all parts of their three-dimensional structure be monitored throughout the period of study, which as yet is impossible. Improvements in confocal microscopy may facilitate this process such that changes in the gross morphology of dendritic spines might be followed during the treatments (Keenan *et al.*, 1988; Deitch *et al.*, 1991; Turner *et al.*, 1991; Fine *et al.*, 1991). However, only large spines and those spines with an optimal orientation with respect to the plane of optical sectioning will be suitable for this type of analysis.

Even with improvements in confocal microscopy, reconstruction from serial EM will be required, to obtain accurate measurement of spine dimensions, many of which are below the theoretical limit for resolution by light microscopy. Serial EM is also required to visualize and to measure the dimensions of subcellular constituents and synaptic areas. Finally, no approach yet available substitutes for serial EM to elucidate the complex interrelationships between neurons, glia, and synapses of the brain (Peters *et al.*, 1976).

It has long been recognized that sampling synaptic structure in the inhomogeneous neuropil is fraught with serious ambiguities (Braendgaard and Gundersen, 1986). The relative densities of synapses can be grossly distorted by the presence of different neuronal and glial elements even in neighboring fields of the same tissue section. The pre- and postsynaptic elements often cannot be identified on single sections. In many brain regions there is a large variability in nearly every aspect of synaptic and dendritic spine morphology. This variability makes it impossible to determine the size, shape, or relative distributions of synapses and spines having different morphologies on single thin sections (Hamlyn, 1962; Westrum and Blackstad, 1962; Andersen *et al.*, 1987a,b; Harris and Stevens, 1989; Harris *et al.*, 1989, 1992). Therefore, the labor-intensive approach involving serial EM is required to obtain accurate identification

of synapses, quantitation of their relative frequencies in the neuropil, and complete measurement of their dimensions.

Serial EM of individual structures in the neuropil by itself is also not adequate because there is no way to determine whether the structures chosen for reconstruction are representative of the population in the neuropil, or are chosen because their unusual characteristics "catch the eye" of the electron microscopist. Therefore, a new approach has been developed, the series sample analysis, which combines serial EM with unbiased sampling and corrections for neuropil inhomogeneities to overcome these ambiguities (Harris *et al.*, 1992).

In the next section of this chapter we describe methods of serial EM and the steps of the series sample analysis. We developed the series sample analysis so that an unbiased sample of structures from the neuropil could be obtained for reconstruction in three dimensions. The second section of this chapter discusses caveats associated with the accuracy of measurements obtained from the three-dimensional reconstructions utilizing serial EM. In both sections we summarize some of the results that have been obtained through the combination of the series sample analysis and three-dimensional reconstructions. Although this chapter focuses primarily on an analysis of synapses and dendritic spines, the same approach can be used more generally to evaluate the relative frequencies, distributions, and three-dimensional structure of any constituent in the neuropil of the brain or more generally of any other subject studied by EM.

## II. SERIES SAMPLE ANALYSIS

### A. Serial Electron Microscopy

Preparation of the tissue for electron microscopy should be optimized for the structure that will be studied (e.g., Jensen and Harris, 1989; Harris *et al.*, 1992). Blocks with embedded tissue are trimmed to contain the entire region of interest, for example, hippocampal CA1 field from the pyramidal cells through the entire apical dendritic arbor (Fig. 18.1a). The trapezoids are serially thin sectioned and the sections are mounted on Formvar-coated or pioliform-coated slot grids (SPI, and Synaptek, Pella) and stained for 5 min with Reynolds' lead citrate. Each grid of each series is then mounted into a gimbal that has been designed specifically for the rotational side entry holder of the JEOL (Tokyo, Japan) 1200EX electron microscope (JEOL SRH-10Mod), and stored in a numbered gelatin capsule.

At the time of photography at the electron microscope, the gimbals are mounted on the rotating stage to obtain consistent orientation of sections

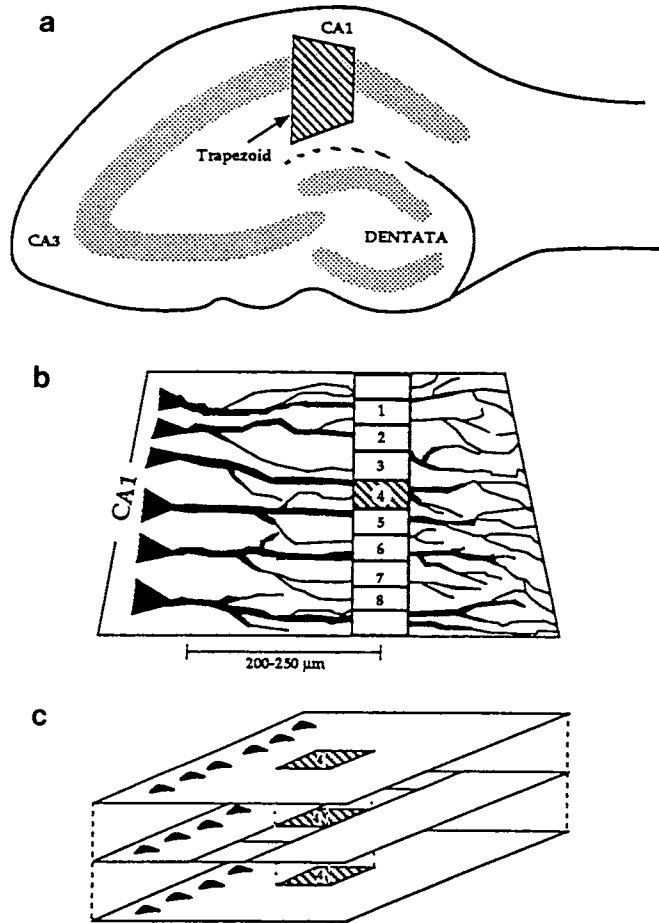


**Fig. 18.1.** Approach for obtaining serial photographs of a well-specified region of neuropil and an unbiased sample from that neuropil: (a) Position the trapezoid relative to known landmarks. (b) Orient the section at the electron microscope and measure from the landmark (e.g., cell bodies) to the region that will be sampled. Divide the sample region into equal sample areas and consult a random number table to determine which region to photograph through serial sections. (c) Photograph through enough serial sections to obtain the largest of the subjects of interest.

on adjacent grids. The sections are rotated to position the bottom of the trapezoid parallel to the edge of the EM photographic screen. The photographic screen is measured at the desired magnification with a calibration grid. Then the region of interest is located by measuring the distance from a known anatomical landmark, such as a cell body layer, with the calibrated photographic screen (Fig. 18.1b). The region of interest is divided

into an equal number of photographic fields and a random number table is consulted to determine which field to photograph through serial sections (Fig. 18.1c). The photographic field is  $500 \mu\text{m}^2$  and the sample area is  $200 \mu\text{m}^2$ , located in the middle of the photographic field on a central reference section. The sample field is smaller than the photographic field to allow for slight shifts in the positioning of the sections while photographing at the electron microscope. These shifts could result in loss of sample structures at the edge of some serial micrographs if all  $500 \mu\text{m}^2$  was analyzed.

A test series of the largest subjects of interest is done to determine the maximum number of sections that must be photographed to contain them. Because the structures transected by the central reference section continue on sections either preceding it and/or following it in the series, a sufficient number of sections must be photographed on both sides of the reference section to contain the subject of interest. For example, in our first study (Harris *et al.*, 1992) we found that 27 serial sections were sufficient to make an unambiguous identification of all but 2 dendritic spines in the sample fields. However, 35 serial sections were required to contain the largest dendritic spines.

## B. Quantitative Series Sample Analysis

A series sample analysis of synapses and dendritic spines involves three steps.

1. Determine the area of homogeneous neuropil by eliminating the sectioned areas of elements in the neuropil that occur nonuniformly (e.g., neuronal and glial cell bodies, large dendritic processes, myelinated axons, and artifacts).

2. Identify every synapse transected by the middle reference section as axodendritic, axospinous, or axosomal, and as asymmetric or symmetric, by viewing them through serial sections. Dendritic spines are further classified into four shape categories that are distinguished by dimensions that could alter their electrotonic effect on synaptic transmission or molecular compartmentalization.

3. Compute the synaptic densities per unit area of homogeneous neuropil and then adjust for differences in the size or shape of the synapses that would influence the probability of viewing them on the reference section. A similar approach could be used to evaluate the relative proportion of the neuropil containing any structure of interest ranging from the cellular to the subcellular to the frequency of structures labeled for a specific molecule.

### ***1. Homogeneous Neuropil Area Calculations***

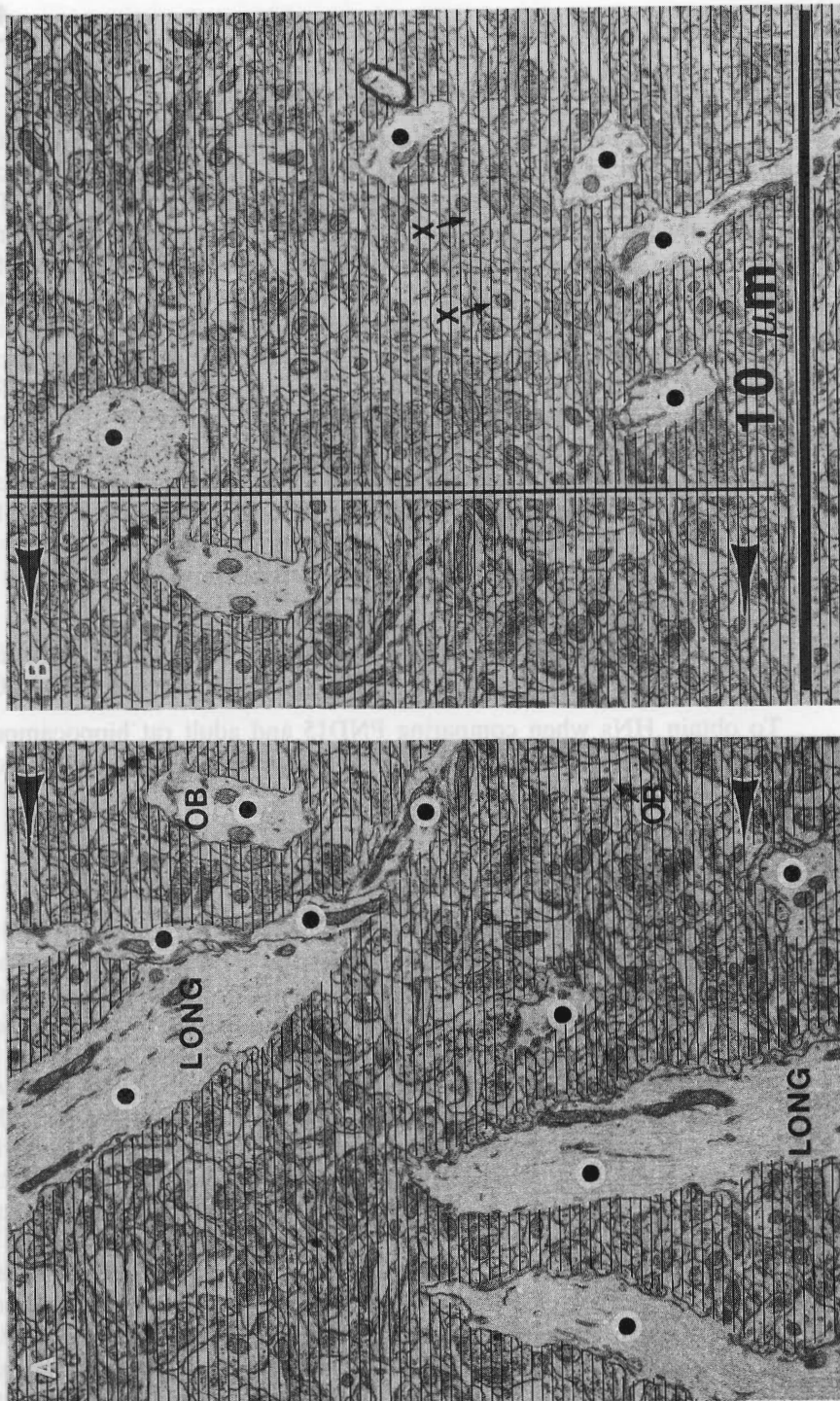
Adjacent sample fields in the neuropil often have different structural components occupying the neuropil (Fig. 18.2). Where possible, cell bodies and blood vessels are excluded from the photographic field. The areas of myelinated axons (MAs) and portions of cell bodies (CBs) not originally recognized in the electron microscope are traced and subtracted from the total sample area. Most of the remaining neuropil contains structures that are part of the synaptic complex, including axons, dendritic spines, and dendritic processes. However, dendritic processes cut parallel or obliquely to their longitudinal axis occur nonuniformly across different sample fields. To establish which of these dendritic processes contribute to the inhomogeneity of the neuropil, the area of every dendritic process on each sample field is measured. Then dendritic process areas are excluded from the total populations of dendrites until all sample fields have a normal distribution of dendritic process areas and homogeneity of variance in this distribution. The homogeneous neuropil area (HN) can be calculated for each sample field:

$$\text{HN} = \text{Total area of the sample field} - \text{areas of the excluded dendritic processes, MA, CB}$$

To obtain HNs when comparing PND15 and adult rat hippocampus, dendritic segment areas greater than  $0.94 \mu\text{m}^2$  needed to be excluded from the sample area (Harris *et al.*, 1992).

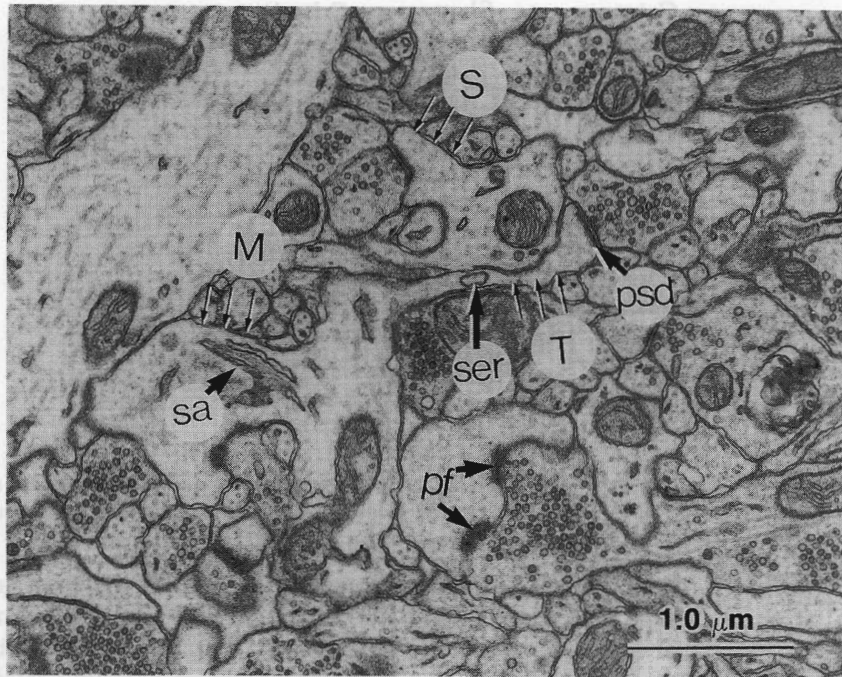
### ***2. Identification of Postsynaptic Elements in Sample Fields***

Every synapse with a portion of its PSD located on the sample field of the reference section is viewed through adjacent serial sections. The postsynaptic element (dendritic shaft, dendritic spine, or cell body) associated with each synapse is identified by viewing it through adjacent serial sections. The asymmetric, presumably excitatory, synapses are identified by a thickened postsynaptic density and round, clear presynaptic vesicles. The symmetric, presumably inhibitory, synapses are identified by a thin pre- and postsynaptic density and pleomorphic vesicles, that is, vesicles with round or flattened shapes. As indicated above, only in the rare fortuitous sections are dendritic spines transected along their longitudinal axis such that a good guess regarding their three-dimensional shapes can be made (Fig. 18.3). However, most dendritic spines on the reference sections cannot be identified until they are viewed through serial sections. For a series sample analysis, each dendritic spine with a PSD on the reference section is followed through serial sections to their origins and classified by the criteria of Fig. 18.4 into one of four shape categories;



**Fig. 18.2.** Adjacent fields from the same neuropil contain grossly different proportions of large and small sectioned dendritic areas. Homogeneous neuropil area is indicated by the lined areas. Sectioned dendritic areas that were excluded from the HN have black circles in their cytoplasm. (A and B) Adjacent portions of the same sample field; the overlap at the left of the vertical line. Calibration in (B) is for (A) and (B). OB, Obliquely sectioned dendrites; LONG, longitudinally sectioned dendrites; X, cross sectioned dendrites.



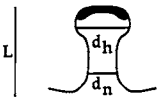
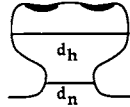
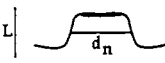
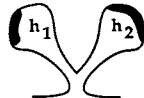


**Fig. 18.3.** Fortuitous section revealing longitudinally sectioned dendritic spines and their subcellular constituents. S, Stubby spine; T, thin spine with a tube of smooth endoplasmic reticulum (ser); M, mushroom spine with a well-laminated spine apparatus (sa); pf, perforated postsynaptic density at the head of a mushroom spine.

thin, mushroom, stubby, or branched. Each dendrite associated with a sample synapse is also identified as spiny or nonspiny by viewing it through adjacent serial sections. Two mushroom-shaped spines from a day-15 rat hippocampus are visualized through serial sections in Fig. 18.5 (Color Section 4). One of these spines was reconstructed. Serial sections were required to identify the spine shapes and distinguish their characteristics. If they had been viewed only on the reference section (section 21), the shape of the yellow spine might have been called either stubby or mushroom, whereas the shape of the pink spine might have been thought to be thin.

### ***3. Correction for Differences in Sizes and Shapes of Synapses That Can Alter Relative Probability of Their Being Transected and Observed on Reference Section***

It has been recognized that the probability of observing part of a PSD on the reference section is proportional to the number of sections that the

Category	Shape	Criteria
Thin		$d_n \ll L$ $d_n \leq d_h$
Mushroom		$d_n \ll d_h$
Stubby		$d_n \cong L$
Branched		> 1 head

**Fig. 18.4.** Categories and criteria by which dendritic spines are assigned to specific shape classes after viewing them on serial thin sections of the series sample.

PSD actually occupies through serial sections (Braendgaard and Gundersen, 1986; Harris *et al.*, 1989, 1992). If PSDs have different sizes, shapes, or orientations relative to the plane of section, the probability of viewing them on the reference section also differs proportionately to the differences in the number of sections they occupy (Fig. 18.6). For example, if an elliptical PSD were sectioned at  $0.07\text{-}\mu\text{m}$  thickness, perpendicular to its short axis with a diameter of  $0.21\ \mu\text{m}$ , three sections of the PSD would be obtained (ellipse labeled 3 in Fig. 18.6). In a 10-section series, with random placement of this PSD in the series, the probability of viewing the PSD on any 1 of the 10 sections is 3 in 10, or 0.3. If the same PSD were sectioned perpendicular to its long axis with a diameter of  $0.42\ \mu\text{m}$ , six sections of the PSD would be obtained (ellipse labeled 6 in Fig. 18.6). Random placement of this PSD in the 10-section series would give a probability of 0.6 of viewing this same PSD in any 1 section, a 100% increase in the probability of counting the same PSD on the reference section. A PSD of the same size as the elliptical PSD, but having an irregular elongated shape that was sectioned across its long axis, could have a probability of being viewed on any 1 section of 10 in 10, or 1 (irregular area labeled 10 in Fig. 18.6). Thus, for the same PSD area there could be a huge range in the probability of counting it on a reference section, depending on its orientation and shape. Furthermore, if the PSD were to decrease in size by a factor of 10, the probability of counting it on the reference section would also be decreased to 0.1, and may be erroneously ascribed to a loss of the synapse rather than to a decrease in its size (Fig. 18.6, small PSD).

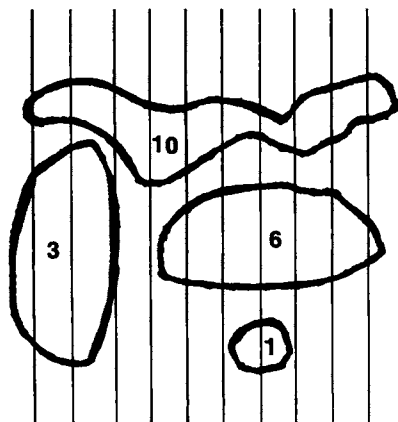


**Fig. 18.6.** Effect of size, shape, and orientation with respect to the plane of sectioning on the number of sections of an object (in this case, postsynaptic densities) sampled. Objects 3, 6, and 10 have the same area, whereas object 1 is one-tenth the area of the other 3 objects. The vertical lines represent equally spaced sections through the objects.

To adjust for these differences in viewing probability, the number of serial sections occupied by each PSD occurring on the reference section is counted. The average number of sections is computed for the PSDs in each synaptic or spine shape category by age, type, and/or experimental condition. Then the following formulas are used to adjust the relative synaptic densities when comparing among the groups.

$$\text{USD (unadjusted synaptic density)} = \frac{\text{number of synapses/neuropil area}}{(\text{NA}; \mu\text{m}^2) \times 100}$$

$$\text{NA} = \text{neuropil area as calculated above}$$

$$\text{ASD (adjusted synaptic density)} = \text{USD} (s'/s)$$

where  $s'$  is the mean number of sections in the categories with the fewest sections and  $s$  is the mean number of sections in the other categories with more sections.

## C. Summary of Results That Have Benefited from Either Partial or Complete Series Sample Analysis

### *1. Dendritic Spines on Spiny Branchlets of Cerebellar Purkinje Cells*

In (Harris and Stevens, 1988) we began by reconstructing all 64 dendritic spines occurring along 2 dendritic segments from Purkinje spiny branchlets. The dimensions of each spine, its PSD, and presynaptic axo-

nal bouton and vesicles were analyzed. The PSD areas were found to be well correlated with other spine and axon dimensions. To determine that the reconstructed spines were representative of a larger population of dendritic spines in the cerebellum, a series sample analysis of an additional 152 PSDs from 4 reference sections was used. This analysis greatly enhanced our confidence that the spines that were reconstructed and measured in three dimensions were not unusual among Purkinje spiny branchlets.

### ***2. Dendritic Spines of Pyramidal Cells in Hippocampal Area CA1***

A similar approach was used to reconstruct 100 dendritic spines along 7 dendritic segments in hippocampal area CA1 (Harris and Stevens, 1989). The dimensions of an additional 465 PSDs obtained through a series sample analysis (Harris *et al.*, 1987, 1992) confirmed that these dendritic spines from young adult hippocampus were not unusual among CA1 dendritic spines.

### ***3. Branched Dendritic Spines at Synapses between Mossy Fibers of Hippocampal CA3 Pyramidal Cells***

In this study (Chicurel and Harris, 1992), a series sample approach was utilized to characterize the subcellular constituents of these complex dendritic spines, to determine the frequency of spines with different numbers of heads, and to evaluate the frequency with which the mossy fibers synapse on different spine heads. Representative dendritic spines with 1, 7, or 12 heads were then randomly selected for complete three-dimensional reconstructions.

### ***4. Comparison of Immature and Mature Dendritic Spines in Hippocampal Area CA1***

The series sample analysis has revealed multiple changes in synaptic, spine, and dendritic structure in stratum radiatum of hippocampal area CA1 between day 15 and adult ages (Harris *et al.*, 1992). The total density of synapses doubles between these ages. However, this doubling does not occur uniformly across spine and synapse morphologies. The number of thin dendritic spines and mushroom dendritic spines with perforated synapses increases four fold, contrasting with the stubby spines that decrease by more than half. The mushroom spines with macular synapses and dendritic shaft synapses have no change in number, and the initially rare branched spines increase in number, and represent about 10% of the total

synapse population in the adult. At day 15 the mushroom and some of the stubby spines had a "prespine apparatus" associated with the spines and sometimes with their synapses. This prespine apparatus consisted of a flattened sheet of smooth endoplasmic reticulum, which in the adults becomes a laminated structure of multiple interconnected cisternae of smooth endoplasmic reticulum (SER) and dense staining material. Three-dimensional reconstructions of individual dendrites coursing through the same neuropil showed that on average the dendritic segments have a similar distribution of different spine shapes along their lengths. Preliminary results from a series sample analysis at day 7 showing most synapses to occur on dendritic shafts (Harris *et al.*, 1989) suggest that spines may differentiate from shaft and stubby spine synapses.

### III. THREE-DIMENSIONAL RECONSTRUCTION FROM SERIAL ELECTRON MICROSCOPY

From the series sample analyses, a subpopulation of dendritic spines can be randomly selected for three-dimensional reconstruction to represent all classes of spines, synapses, dendrites, and so on observed in the neuropil. This random selection eliminates potential selection biases of the investigator. There are, however, other sources of error that could contribute to an invalid estimate of spine, synapse, dendritic, axonal, or other structural dimensions obtained through reconstruction from serial EM. Two of the main sources of error, section thickness and chemical fixation, are addressed here.

#### A. Sources of Error in Three-Dimensional Reconstructions

##### 1. Section Thickness

For a given section, the thickness can vary considerably even across a section of uniform color when floating on the surface of the water (Peachey, 1958). Therefore, it was important to establish a procedure for estimating the section thickness in the region of the section from which the subjects were reconstructed. The section thickness dial is set to between 70 and 100 nm on the ultramicrotome at the time of sectioning, to give an interference color of platinum, that is, between silver and gold, to minimize section folds that occur frequently at silver ( $\sim 70 \mu\text{m}$ ), and to minimize overlapping of adjacent structures, which occurs frequently at gold ( $\sim 90\text{--}100 \mu\text{m}$ ). The range in mechanical setting reflects the sensitivity of this process to air temperature, humidity, and other factors in the

environment. The estimate of section thickness in the field that is photographed is obtained from the electron micrographs by measuring the diameters of the longitudinally sectioned cylindrical mitochondria at their maxima in single sections, and comparing the measured diameter to the number of sections in which the mitochondria appear (Harris and Stevens, 1988, 1989). Section thickness is then calculated:

$$\text{Thickness } (\mu\text{m}/\text{section}) = \text{measured diameter } (\mu\text{m})/\text{number of sections}$$

We have had no evidence that a significant amount of material is lost "between" adjacent sections. There is no buildup of Epon or other substances in the water of the boat, on the diamond knife edge, or between adjacent sections on the grid (Fig. 18.7). On reconstruction, all spines and synapses appear complete when traced throughout the series, further suggesting that no significant material is lost during sectioning. We suggest that this approach provides the best estimate of section thickness that can be readily obtained from each set of serial sections, and that the potential error due to this factor has been minimized.

## ***2. Changes in Tissue Volume Due to Process of Chemical Fixation***

With the present methods, it is impossible to determine whether tissue processing itself alters dendritic spines and their synapses. In one study,

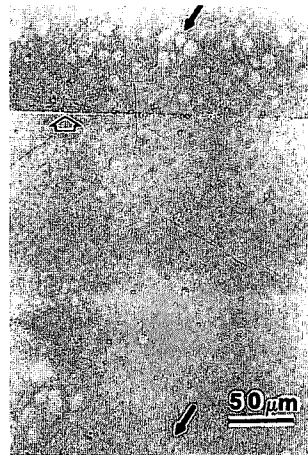


**Fig. 18.7.** Adjacent serial sections reveal no significant loss of material between sections. The open arrow is at the junction between the adjacent sections and the two black arrows point to the same cell on the adjacent sections.

we have compared the cross-sectional areas of mitochondria obtained from perfusion-fixed rats [using 2% (v/v) paraformaldehyde and 2.5% (v/v) glutaraldehyde] with mitochondria in hippocampal slices prepared by rapid immersion fixation in fixative containing 2% (v/v) paraformaldehyde and 6% (v/v) glutaraldehyde and microwave irradiated for 8 sec (Jensen and Harris, 1989). In this procedure, the tissue is exposed to the fixative for less than 1 min, although the concentration of the fixative is much higher than in standard procedures. Even so, no significant differences were found in the cross-sectional areas of the mitochondria under the two conditions, suggesting that at least there is not a generalized swelling response correlated with fixative concentration.

We have also observed the process of fixation in 2% paraformaldehyde and 2.5% glutaraldehyde of hippocampal neurons maintained *in vitro* (K. M. Harris, S. Fischel, and P. A. Rosenberg, unpublished observations). No measurable changes were detected in the dimensions of dendrites or dendritic spinelike processes before, during, or for 1 hr after immersion in the fixative (Fig. 18.8). Confocal microscopy could be used to determine whether these processes undergo changes in their dimensions in the *Z* dimension, which is not well visualized by video-enhanced light microscopy. Until there is specific evidence, however, to suggest that spines and synapses are altered by the tissue processing, we have not introduced a "correction" factor to account for this potential artifact.

## **B. Three-Dimensional Reconstructions of Individual Dendritic Spines and Synapses**

### ***1. Reconstruction Methods***

Subsequent to a series sample analysis, spines in each shape class are randomly selected from the sample fields and reconstructed and graphically edited into neck and head compartments, using the methods described in Harris and Stevens (1988, 1989). The reconstructions involve positioning the EM negatives under a video camera, capturing the positive image in the frame grabber, and then microaligning the adjacent sections by switching between the stored image and the live image and rotating the live image until concurrent *X*, *Y*, and rotational motion is minimized. The perimeter of the plasmalemma of each dendritic spine is traced through serial sections. For sections in which the spines are connected to the parent dendrite, the dendrite is also traced but subsequently removed graphically to ensure the spine origin is properly positioned.

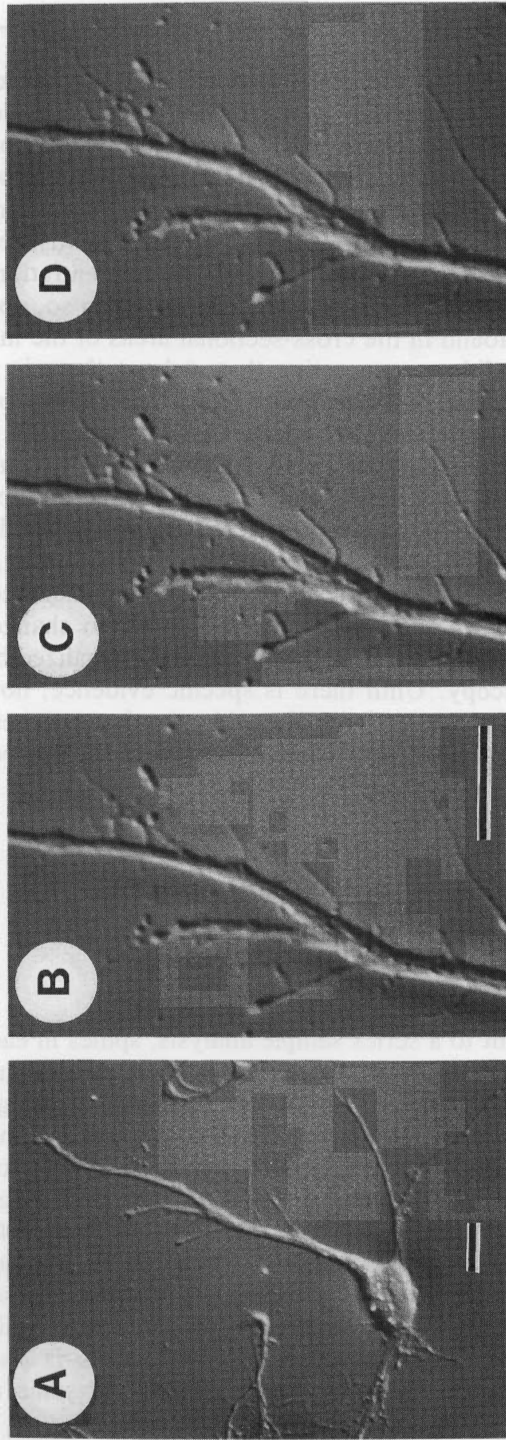


**Fig. 18.8.** Pyramidal-like hippocampal cells in culture that were dissociated on embryonic days 18–20 and allowed to grow *in vitro* for 10 days (K. M. Harris, S. Fischel, and P. A. Rosenber, unpublished observations). (A) Cell viewed with video-enhanced contrast light microscopy and photographed just prior to adding fixative to the culture. (B) High-magnification view of a segment of neurite from the cell (A) just prior to fixation. (C) The same segment of neurite at 1 min 30 sec after adding the fixative, and (D) 20 min after adding the fixative. Bars: 10  $\mu$ m. Bar in (B) is for (B), (C), and (D).



## 2. Quantitation of Dimensions

Volumes are calculated by summing enclosed areas of the cytoplasm across serial sections and multiplying by section thickness. Surface areas are calculated by summing perimeters and multiplying by section thickness across serial sections, and then adding the enclosed areas of tangentially sectioned surfaces of the spine or the postsynaptic density seen on individual sections as gray shadows. The diameters are measured on individual sections of cross-sectioned spines, and along the lengths of longitudinally sectioned spines. The lengths of longitudinally sectioned spine necks and heads are obtained on the section where they are attached to the parent dendrite. For obliquely or cross-sectioned spines, their lengths are computed across serial sections by positioning a length to center a point in the contour, and computing the hypotenuse of a right triangle with the base equal to section thickness and the height equal to the length in each section. These hypotenuses are then summed over adjacent sections. For obliquely sectioned spines, the length at the origin and connection to the head are then added to this sum of hypotenuses. Similar calculations are made for total head length, and/or to the PSD if the PSD is at the side of the head.

For cross-sectioned asymmetric synapses, the area of the PSD is determined by measuring its length through adjacent sections, multiplying the lengths by section thickness, and then adding across sections. For obliquely or tangentially sectioned PSDs, the enclosed area is measured on each section where it appears. If two or more adjacent sections contain oblique or tangential sections of the PSD, a connector is drawn where the contours overlap, and its length is multiplied by section thickness to account for PSD area traversing the sections. The total area of the oblique or tangential PSDs is computed by adding the areas of the closed contours to the area computed through section thickness of the connectors.

## C. Three-Dimensional Reconstructions of Dendritic Segments Coursing through Neuropil

Complete reconstructions of dendritic segments have been obtained to determine the mean density of differing spine and synapse morphologies occurring along individual dendrites in both hippocampus and cerebellum (Harris and Stevens, 1988, 1989; Harris *et al.*, 1992). Following a series sample analysis, all spines and synapses originating from a subpopulation of dendritic segments randomly selected from the reference section are viewed through serial sections to determine their shape and characteris-

tics. The dendritic diameter is measured in each section, and its length measured across serial sections.

To measure the length of cross sectioned or obliquely sectioned dendrites across serial sections, a graphics editor is used to position a point in the center of the dendritic trace on section 1. On subsequent sections lengths are added to maintain a central location for the point. Then the hypotenuse of a right triangle is computed with its base equal to section thickness, and the height equal to the length required to maintain the connecting point in the center of the dendritic trace. Wherever the dendritic segment is perfectly cross sectioned the hypotenuse equals the base, that is, 1 section in thickness. The total length of the dendritic segment equals the sum of the hypotenuses across all of the serial sections.

Complete reconstructions of dendritic segments have been obtained to determine if the mean density of the different types of synapses occurring along these dendrites is reflected accurately in a series sample analysis of the neuropil. Alternatively, dendrites from a particular age or treatment group could be heterogeneous in spine and synapse densities. Then the mean differences in the sample fields would not accurately reflect differences along the individual dendrites. On both day 15 and young adult ages in the rat hippocampal area CA1, the series sample analysis usually reflects the relative distribution of spines along the individual dendrites coursing through the neuropil. However, isolated dendrites could be found that had a predominance of one spine shape over others (Harris *et al.*, 1992).

These complete dendritic reconstructions reveal the number of spines, distribution of spine shapes, and whether spines tend to cluster or be uniformly distributed along the dendrites (Fig. 18.9, Color Section 4). Depending on the orientation of the dendrite with respect to the optical sectioning plane, the presence of the large dendritic shaft and near-neighbor overlap of dendritic spines, not to mention possible incomplete filling of the small spines, could confound interpretation of the images from confocal microscopy. In addition, the accuracy of reconstructions obtained from confocal images through dendritic spines will be proportional to the number of sections that can be obtained, just as it is with serial EM. Using serial EM and section thicknesses of around  $0.07\ \mu\text{m}$ , spines ranging from  $0.5$  to  $2\ \mu\text{m}$  in length can be sampled in 7 to 28 serial sections. With current methods, the sampling rate from confocal microscopy would be from one or two sections to four sections for the same spine. If the spines have complex morphologies, this low sampling rate could easily miss important variation in spine geometry and dimensions, and therefore images from confocal microscopy should be interpreted with great caution.

### D. Summary of Results from Three-Dimensional Reconstructions of Dendritic Spines and Synapses

To distinguish the features that are common from those that are unusual among spines with different functions, the complete three-dimensional reconstructions from serial EM have been used to compare the dendritic spines in the cerebellum and hippocampal areas CA1 and CA3 (Harris and Stevens, 1988, 1989; Chicurel and Harris, 1989, 1992). Some of the findings from these studies are summarized in Table I. Note that for the purposes of this summary the term *synapse* comprises the presynaptic axonal bouton, its postsynaptic partner, and the dense-staining material of the synaptic cleft and postsynaptic densities.

For most spines one set of axonal vesicles apposes a single postsynaptic density, although sharing of vesicles in a presynaptic varicosity is not uncommon. In hippocampal area CA1, for example, about 25% of the CA3 axonal boutons are shared by at least two dendritic spines (Sorra and Harris, 1991). In the cerebellum, 27% of the axonal boutons of the parallel fibers are shared by more than one dendritic spine, and most of this sharing occurs among neighboring spines of the same dendritic segment (Harris and Stevens, 1988). In hippocampal area CA3, the mossy fiber boutons always synapse with more than one spine head, and we have encountered as many as 37 spine heads from 7 different branched spines synapsing with 1 mossy fiber bouton (Chicurel and Harris, 1989, 1992).

The PSD occupies about 10% of the spine head surface area and usually there is one PSD per spine head. In contrast, some heads of branched

**TABLE I**  
Structural Features of Dendritic Spines

Feature	Typical appearance	Unusual appearance
Axonal vesicles	One set per synapse; number proportional to size of synapse	One set shared by >1 synapse
PSD	One asymmetric on spine head Macular, continuous area proportional to number of axonal vesicles; 10–15% of head area	Some branches with none, some symmetric on necks; irregular, perforated
Head	One per spine neck, small and spherical; size proportional to number of axonal vesicles, PSD, and subcellular constituents	Branched, large and irregular
Neck	Cylindrical; do not reduce charge transfer	Absent or branched
Subcellular constituents	Single or branched tube of SER	Spine apparatus, ribosomes, microtubules, multivesicular bodies, mitochondria, spinules

spines have no synapse on them, and some spines in other brain regions frequently have symmetric, presumably inhibitory, synapses on the spine neck in addition to the asymmetric PSDs on the spine heads (Colonnier, 1968; Peters *et al.*, 1976; DiFiglia *et al.*, 1982). The PSD of most spines is continuous and its size is proportional to the number of vesicles in the presynaptic axonal varicosity.

Most spines have a small, nearly spherical head with a volume that is proportional to the area of the PSD. It is not uncommon, however, for spine heads to assume a large, irregular shape with a highly irregular PSD containing perforations that can cause the PSD to be segmented into discrete islands on the spine heads. The necks of most spines are approximately cylindrical and are not long or constricted enough to alter the transfer of charge from the synapse to the postsynaptic dendrite. Nearly all spines contain some smooth endoplasmic reticulum with a volume that is proportional to the spine volume. Unusually complex spines contain a spine apparatus, mitochondria, ribosomes, and microtubules.

### **E. Implications of Spine Dimensions and Three-Dimensional Characteristics for Spine Function**

These three-dimensional studies combined with standard biophysical models of spine geometry in the cerebellum and hippocampus have led to several viable hypotheses about the functions of dendritic spine geometry in these brain regions (Fig. 18.10). Although most of the excitatory synapses in the CNS occur on dendritic spines, it is unlikely that excitatory synaptic transmission is modulated through local inhibition of the spines in cerebellum or hippocampal areas CA1 and CA3, because symmetric inhibitory synapses rarely occur on their spine necks (Fig. 18.10a; Harris and Stevens, 1988, 1989; Chicurel and Harris, 1992; Sorra and Harris, 1991; Harris *et al.*, 1992).

From both an ontogenetic and an evolutionary viewpoint, dendritic spines could conserve brain volume and allow more synapses to interdigitate in a restricted brain volume (Fig. 18.10b). Alternatively, the dendrites could have just become thinner to pack more synapses in a given brain volume without the formation of dendritic spines. Two lines of evidence support the first hypothesis. First, as dendrites elongate and dendritic spines form during hippocampal maturation, the parent dendritic shafts become thinner, suggesting that the original dendritic cytoplasm was used to create the dendritic spines (Harris *et al.*, 1989, 1992). Second, in all the brain regions from which spines have been reconstructed to date, the synapse, as delineated by the PSD, consistently occupies only about 10%

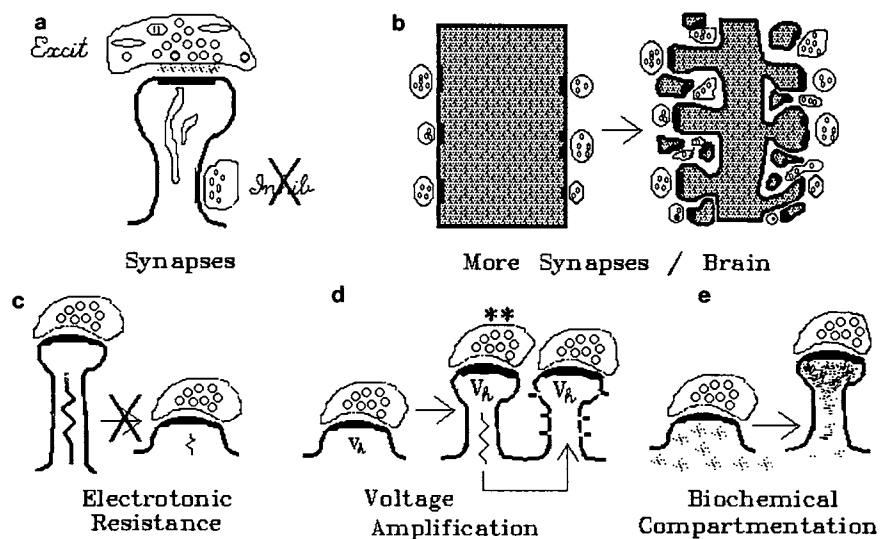


**Fig. 18.10.** Possible functions of dendritic spines in hippocampal area CA1 and cerebellar cortex. For detailed explanations see text.

of the spine head surface area (Harris and Stevens, 1988, 1989; Chicurel and Harris, 1989; Spacek, 1983; Wilson *et al.*, 1983). This roughly 10% occupancy by the PSD is also true for developing dendritic spines (Harris *et al.*, 1989, 1992). Thus, synapses may require a minimum area of non-synaptic membrane to accommodate other important molecules that are not found in the PSD. Conservation of brain volume through reduction in the dendritic component, without loss of nonsynaptic membrane area, could be achieved only by forming dendritic spine-like projections.

Two lines of evidence suggest that dendritic spines do not modulate synaptic efficacy by altering electrotonic resistance to charge transfer through their necks (Fig. 18.10c). First, adult cerebellar and hippocampal dendritic spine necks are not sufficiently thin to reduce charge transfer, and thus widening their necks is unlikely to enhance charge transfer (Harris and Stevens, 1988, 1989; Chicurel and Harris, 1989). Second, spine necks constrict, not widen, with the maturation of enhanced synaptic efficacy (Mates and Lund, 1983; Harris *et al.*, 1989, 1992). Spine neck constriction is consistent with a role for voltage amplification at the synapse (Fig. 18.10d) and with an enhanced compartmentalization of specific molecules at the synapse (Fig. 18.10e; Wilson *et al.*, 1983; Wilson, 1984; Harris and Stevens, 1988, 1989; Brown *et al.*, 1988; Wickens, 1988; Zador *et al.*, 1990).

#### IV. SUMMARY AND CAUTIONS

We have illustrated the power of serial EM to elucidate the dimensions of dendritic spines and the relative frequencies of spines and synapses with different morphologies in a random sample of the neuropil. This approach is extremely useful in providing the detailed descriptions about the interrelationships between spine geometry, synaptic morphology, and their subcellular constituents; all features that are necessary to make accurate predictions about the effect of spine structure on synaptic function. However, this approach does not allow the life history of an individual dendritic spine to be monitored. Confocal microscopy may allow for some of the gross changes in spine geometry to be monitored. If properly combined with serial EM it could hold promise for understanding how changes in spine morphology might modulate synaptic function, and vice versa.

#### REFERENCES

- Andersen, P., Blackstad, T., Hulleberg, G., Trommald, M., and Vaaland, J. L. (1987a). Dimensions of dendritic spines of rat dentate granule cells during long-term potentiation (LTP). *J. Physiol. (London)* **390**, 264.
- Andersen, P., Blackstad, T., Hulleberg, G., Vaaland, J. L., and Trommald, M. (1987b). Changes in spine morphology associated with LTP in rat dentate granule cells. *Proc. Physiol. Soc.* **PC50**, 288P.
- Baer, S. M., and Rinzel, J. (1991). Propagation of dendritic spikes mediated by excitable spines: A continuum theory. *J. Neurophysiol.* **65**, 874–890.
- Blackstad, T. W., and Kjaerheim, A. (1961). Special axo-dendritic synapses in the hippocampal cortex: Electron and light microscopic studies in the layer of mossy fibers. *J. Comp. Neurol.* **117**, 133–159.
- Braendgaard, H., and Gundersen, H. J. (1986). The impact of recent stereological advances on quantitative studies of the nervous system. *J. Neurosci. Methods* **18**, 39–78.
- Brown, T. H., Chang, V. C., Ganong, A. H., Keenan, C. L., and Kelso, S. R. (1988). Biophysical properties of dendrites and spines that may control the induction and expression of long-term synaptic potentiation. *Neurol. Neurobiol.* **35**, 201–264.
- Chicurel, M. E., and Harris, K. M. (1989). Serial electron microscopy of CA3 dendritic spines synapsing with mossy fibers of rat hippocampus. *Soc. Neurosci. Abstr.* **15**, 256.
- Chicurel, M. E., and Harris, K. M. (1992). Three dimensional analysis of the structure and composition of CA3 branched dendritic spines and their synaptic relationships with mossy fiber boutons in the rat hippocampus. *J. Comp. Neurol.* **325**, 169–182.

- Colonnier, M. (1968). Synaptic patterns on different cell types in the different laminae of the cat visual cortex. An electron microscope study. *Brain Res.* **9**, 268–287.
- Coss, R. G., and Perkel, D. H. (1985). The function of dendritic spines: A review of theoretical issues. *Behav. Neural Biol.* **44**, 151–185.
- Deitch, J. S., Smith, K. L., Swann, J. W., and Turner, J. N. (1991). Ultrastructural investigation of neurons identified and localized using the confocal scanning laser microscope. *J. Electron Microsc. Tech.* **18**, 82–90.
- Desmond, N. L., and Levy, W. B. (1990). Morphological correlates of long-term potentiation imply the modification of existing synapses, not synaptogenesis, in the hippocampal dentate gyrus. *Synapse* **5**, 139–143.
- Diamond, J., Gray, E. G., and Yasargil, G. M. (1970). The function of the dendritic spine: An hypothesis. In "Excitatory Synaptic Mechanisms" (P. Andersen and J. K. S. Jensen, eds.), pp. 213–222. Universitets Forlaget, Oslo, Norway.
- DiFiglia, M., Aronin, N., and Martin, J. B. (1982). Light and electron microscopic localization of immunoreactive Leu-enkephalin in the monkey basal ganglia. *J. Neurosci.* **2**, 303–320.
- Fine, A., Hosakawa, T., and Bliss, T. V. P. (1991). Confocal imaging of changes in synaptic structure in living hippocampal slices. *Soc. Neurosci. Abstr.* **17**, 1328 (abstr).
- Gamble, E., and Koch, C. (1987). The dynamics of free calcium in dendritic spines in response to repetitive synaptic input. *Science* **236**, 1311–1315.
- Gray, E. G. (1959). Axo-somatic and axo-dendritic synapses of the cerebral cortex: An electron microscopic study. *J. Anat.* **93**, 420–433.
- Greenough, W. T., and Bailey, C. H. (1988). The anatomy of a memory: Convergence of results across a diversity of tests. *Trends Neurosci.* **11**, 142–147.
- Hamlyn, L. H. (1962). The fine structure of the mossy fibre endings in the hippocampus of the rabbit. *J. Anat.* **96**, 112–120.
- Harris, K. M., and Stevens, J. K. (1988). Dendritic spines of rat cerebellar Purkinje cells: Serial electron microscopy with reference to their biophysical characteristics. *J. Neurosci.* **8**, 4455–4469.
- Harris, K. M., and Stevens, J. K. (1989). Dendritic spines of CA1 pyramidal cells in the rat hippocampus: Serial electron microscopy with reference to their biophysical characteristics. *J. Neurosci.* **9**, 2982–2997.
- Harris, K. M., Jensen, F. E., and Tsao, B. (1987). Development of hippocampal synapses, spines, and LTP. *Soc. Neurosci. Abstr.* **13**, 1429 (abst).
- Harris, K. M., Jensen, F. E., and Tsao, B. (1989). Ultrastructure, development, and plasticity of dendritic spine synapses in area CA1 of the rat hippocampus: Extending our vision with serial electron microscopy and three-dimensional analyses. *Neurol. Neurobiol.* **52**, 33–52.
- Harris, K. M., Jensen, F. E., and Tsao, B. (1992). Three-dimensional structure of dendritic spines and synapses in rat hippocampus (CA1) at postnatal day 15 and adult ages: Implications for the maturation of synaptic physiology and long-term potentiation. *J. Neurosci.* **12**, 2686–2705.

- Jensen, F. E., and Harris, K. M. (1989). Preservation of neuronal ultrastructure in hippocampal slices using rapid microwave-enhanced fixation. *J. Neurosci. Methods* **29**, 217–230.
- Jones, E. G., and Powell, T. P. S. (1969). Morphological variations in the dendritic spines of the neocortex. *J. Cell Sci.* **5**, 509–529.
- Kawato, M., and Tsukahara, N. (1983). Theoretical study on electrical properties of dendritic spines. *J. Theor. Biol.* **103**, 507–522.
- Keenan, C. L., Chapman, P. F., Chang, V. C., and Brown, T. H. (1988). Videomicroscopy of acute brain slices from amygdala and hippocampus. *Brain Res. Bull.* **21**, 373–383.
- Koch, C., and Poggio, T. (1983). Electrical properties of dendritic spines. *Trends Neurosci.* **6**, 80–83.
- Mates, L. S., and Lund, J. S. (1983). Spine formation and maturation of type-I synapses on spiny stellate neurons in primate visual cortex. *J. Comp. Neur.* **221**, 91–97.
- Muller, W., and Connor, J. A. (1991). Dendritic spines as individual neuronal compartments for synaptic  $CA^{2+}$  responses. *Nature (London)* **354**, 73–76.
- Peachey, L. D. (1958). A study of section thickness and physical distortion produced during microtomy. *J. Biophys. Biochem. Cytol.* **4**, 233–242.
- Peters, A., and Kaiserman-Abramof, I. R. (1970). The small pyramidal neuron of the rat cerebral cortex. The perikaryon, dendrites and spines. *J. Anat.* **127**, 321–356.
- Peters, A., Palay, S. L., and Webster, H. def. (1976). “The Fine Structure of the Nervous System: The Neurons and Supporting Cells.” Saunders, Philadelphia.
- Purpura, D. P. (1974). Dendritic spine “dysgenesis” and mental retardation. *Science* **186**, 1126–1128.
- Purpura, D. P. (1975a). Normal and aberrant neuronal development in the cerebral cortex of human fetus and young infant. In “Brain Mechanisms in Mental Retardation” (N. A. Buchwald and M. A. B. Brazier, eds.), pp. 141–170. Academic Press, New York.
- Purpura, D. P. (1975b). Dendritic differentiation in human cerebral cortex: Normal and aberrant developmental patterns. In “Physiology and Pathology of Dendrites” (G. W. Kretzberg, ed.), pp. 91–116. Raven Press, New York.
- Rall, W. (1970). Cable properties of dendrites and effects of synaptic location. In “Excitatory Synaptic Mechanisms” (P. Andersen and J. K. S. Jensen, eds.), pp. 175–187. Universitets Forlaget, Oslo, Norway.
- Rall, W. (1974). Dendritic spines, synaptic potency, and neuronal plasticity. In “Cellular Mechanisms Subservicing Changes in Neuronal Activity” (C. Woody, K. Brown, T. Crow, and J. Knispel, eds.), pp. 13–21. Brain Information Service, Los Angeles.
- Rall, W. (1977). Core conductor theory and cable properties of neurons. In “Handbook of Physiology” (E. R. Kandel, ed.), Sect. 1, Vol. II, pp. 39–97. Am. Physiol. Soc., Bethesda, MD.
- Rall, W. (1978). Dendritic spines and synaptic potency. In “Studies in Neurophysiology” (A. K. McIntyre and K. Porter, eds.), pp. 203–209. Cambridge Univ. Press, Cambridge.



- Ramón Y Cajál S (1893) Neue Darstellung vom Histologischen Bau des Centralnervensystems. *Arch. Anat. Entwicklungsgesch. Anatom. Abt. Arch. Anat. Physiol.*, 319–428.
- Redman, S. (1990). Quantal analysis of synaptic potentials in neurons of the central nervous system. *Physiol. Rev.* **70**, 165–198.
- Scheibel, M. E., and Scheibel, A. B. (1968). On the nature of dendritic spines: Report of a workshop. *Comm. Behav. Biol.* **A1**, 231–265.
- Schuz, A. (1978). Some facts and hypotheses concerning dendritic spines and learning. In “Architectonics of the Cerebral Cortex” (M. A. B. Brazier and H. Petsche, eds), pp. 129–135. Raven Press, New York.
- Segev, I., and Rall, W. (1988). Computational study of an excitable dendritic spine. *J. Neurophysiol.* **60**, 499–523.
- Sorra, K. E., and Harris, K. M. (1991). Multiple contacts between hippocampal CA3 axons and apical dendrites of CA1 pyramidal cells. *Soc. Neurosci. Abstr.* **17**, 1156, (abst.).
- Spacek, I. and Hartmann, M. (1983). Three-dimensional analysis of dendritic spines: I. Quantitative observations related to dendritic spine and synaptic morphology in cerebral and cerebellar cortices. *Anat. Embryol.* **167**, 289–310.
- Tanzi, E. (1893). I Fatti i le induzioni nell’odierna istologia del sistema nervoso. *Riv. Sper. Freniatr. Leg. Alienazioni Ment.* **19**, 419–472.
- Turner, D. A. (1988). Waveform and amplitude characteristics of evoked responses to dendritic stimulation of CA1 guinea-pig pyramidal cells. *J. Physiol. (London)* **395**, 419–439.
- Turner, J. N. Szarowski, D. H., Smith, K. L., Marko, M., Lenth, A., and Swann J. W. (1991). Confocal microscopy and three-dimensional reconstruction of electrophysiologically identified neurons in thick brain slices. *J. Electron. Microsc. Tech.* **18**, 11–23.
- Wallace, C., Hawrylak, N., and Greenough, W. T. (1991). Studies of synaptic structural modifications after long-term potentiation and kindling: Context for a molecular morphology. In “Long-term Potentiation: A Debate of Current Issues” (M. Baudry and J. L. Davis, eds.), pp. 189–232. MIT Press, Cambridge, MA.
- Westrum, L. E., and Blackstad, T. (1962). An electron microscopic study of the stratum radiatum of the rat hippocampus (regio superior, CA1) with particular emphasis on synaptology. *J. Comp. Neur.* **119**, 281–309.
- Wickens, J. (1988). Electrically coupled but chemically isolated synapses: Dendritic spines and calcium in a rule for synaptic modification. *Prog. Neurobiol.* **31**, 507–528.
- Wilson, C. J. (1984). Passive cable properties of dendritic spines and spiny neurons. *J. Neurosci.* **4**, 281–297.
- Wilson, C. J., Groves, P. M., Kitai, S. T., and Linder, J. C. (1983). Three dimensional structure of dendritic spines in rat striatum. *J. Neurosci.* **3**, 383–398.
- Zador, A., Koch, C., and Brown, T. H. (1990). Biophysical model of a Hebbian synapse. *Proc. Natl. Acad. Sci. U. S. A.* **87**, 6718–6722.

## COLOR SECTION 4

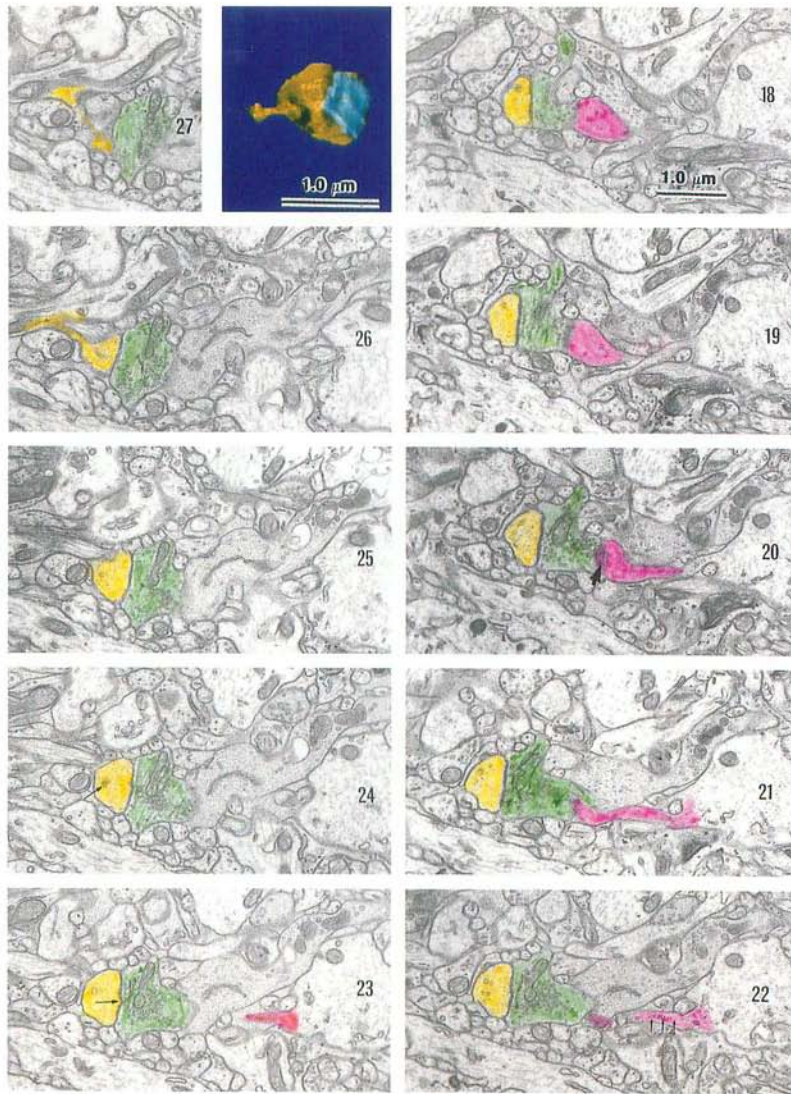


**Fig. 18.5.** Serial sections through two dendritic spines that are in the same shape category (mushroom), but that have different appearances in some of the sections. The reconstruction is of the spine whose cut portions are colored yellow on a subset of the serial sections that contain it. The second spine, colored pink, shares the presynaptic axonal bouton (colored green) with the first spine. Section numbers are labeled on the right side of each micrograph. The arrow in section 24 points to a portion of a tube of smooth endoplasmic reticulum. The arrow in section 23 points to a tiny perforation in the PSD. The row of small arrows in section 22 indicates polyribosomes in the neck of the “pink” spine, and the large arrow in section 20 indicates an obliquely sectioned PSD on the “pink” spine.

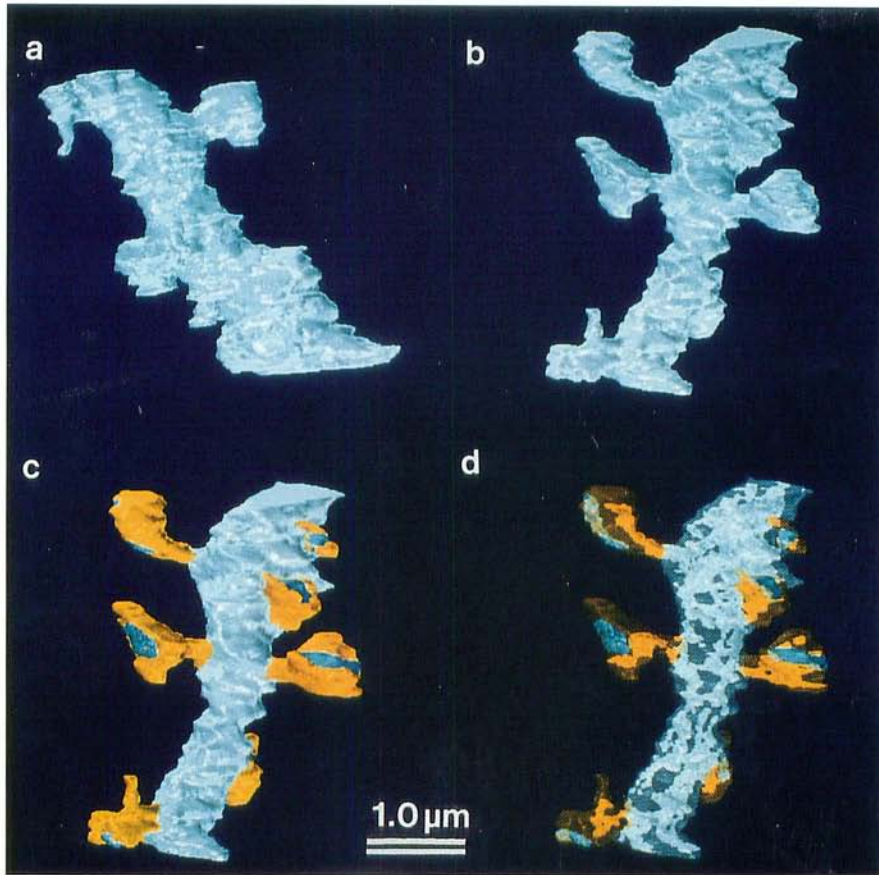


**Fig. 18.9.** Reconstruction of a dendritic segment in hippocampal area CA1. (a) A viewing angle of the dendritic segment whose spines are obscured by the parent dendrite and each other. Were this viewing angle obtained in the light microscope only one dendritic spine would be accurately discerned. (b) A different viewing angle of the same dendritic segment reveals three or four spines at their optimal viewing angles. (c) Each dendritic spine is displayed in yellow, with the location of the synapse identified by a complete reconstruction in blue of the postsynaptic densities. (d) The same dendritic segment with the spines and dendritic segment transparent so that the distribution of the smooth endoplasmic reticulum within the spine and dendrite can be seen. Bar: 1  $\mu\text{m}$ .